J. Synchrotron Rad. (1998). **5**, 940–942

High-energy magnetic Compton scattering experiments at ESRF

Th. Tschentscher,[a]* J. E. McCarthy,[a,b] V. Honkimäki[a,c] and P. Suortti[a]

[a]*European Synchrotron Radiation Facility, BP 220, F-38043 Grenoble CEDEX, France,* [b]*Department of Physics, University of Warwick, Coventry CV4 7AL, England, and* [c]*Department of Physics, University of Helsinki, FIN-00014 University of Helsinki, Finland.*
E-mail: thomas.tschentscher@desy.de

(*Received 4 August 1997; accepted 21 November 1997*)

Investigations of spin densities in ferromagnetic materials using magnetic Compton scattering are reported. At the high-energy beamline ID15 at the ESRF, experiments have been carried out utilizing the high flux at very high photon energies. Energies from 60 up to 1000 keV have been used for investigations of experimental resolution, cross section, spin moments and momentum distribution. Optimized conditions are found for photon energies from 200 to 250 keV with a momentum resolution < 0.4 a.u. and a doubled magnetic effect compared with earlier measurements. In the determination of absolute spin moments multiple scattering has to be taken into account.

Keywords: magnetic Compton scattering; high-energy synchrotron radiation; spin densities; ferromagnets; multiple scattering.

1. Introduction

In inelastic Compton scattering with circularly polarized photons the scattering does not solely arise from the electron charge but also from the magnetic moment due to the electron spin. This was recognized early on (Platzman & Tzoar, 1970) and the first experiments were carried out using radioisotopes emitting circular polarized γ-radiation (Sakai & Ôno, 1976). To achieve higher photon flux the experiments were later transferred to synchrotron radiation sources (Cooper *et al.*, 1988) and carried out at photon energies around 60 keV. Recently the use of higher photon energies became possible, which leads to an increase of the magnetic effect, to an improvement of the resolution and which enables measurements on high-Z materials. A recent review of magnetic Compton scattering is given by Sakai (1996). The high-energy beamline ID15 at ESRF is dedicated to the use of high-energy photons and is optimized for a high flux of circularly polarized photons. Magnetic Compton scattering is one field of research at this beamline (Suortti & Tschentscher, 1995; Tschentscher & Suortti, 1998) and its major achievements and results from experiments at high photon energies will be presented in this paper. Measurements of magnetic Compton profiles using the high-resolution spectrometer at an energy of 60 keV will be reported in a forthcoming publication (McCarthy Honkimäki *et al.*, 1998).

2. Magnetic Compton profiles

It is well established that magnetic Compton scattering is sensitive only to the electron spin moment and disregards the orbital moment (Cooper *et al.*, 1992; Carra *et al.*, 1996). In combination with measurements of the total moment one obtains information about spin and orbital contributions to the magnetic moment. Because Compton scattering averages over all electrons, only ferro- or ferrimagnets can be investigated. The size of the magnetic signal obtained from the sample is proportional to the total magnetic spin moment S, and the shape of the magnetic Compton profile $J_{\rm mag}(p_z)$ reflects the distribution of spin density in momentum space.

$$J_{\rm mag}(p_z) = \int [n\uparrow(p) - n\downarrow(p)]{\rm d}p_x{\rm d}p_y$$

and

$$S = \mu_{\rm B} \int J_{\rm mag}(p_z){\rm d}p_z \qquad (1)$$

$\mu_{\rm B}$ is the Bohr magneton and $J_{\rm mag}(p_z)$ corresponds to the difference between the experimental signals obtained by inverting the sign of σP_c, where σ corresponds to the direction of magnetization of the sample and the Stokes parameter P_c describes the helicity of the beam. At the photon energies of interest the sign is usually flipped by inverting the sample magnetization. The high stability of the photon beam at the ESRF would make it possible to invert the helicity of the incident photons by selecting photons above or below the beam center with a slit system. This scheme had been tested, but results were not conclusive because of the difficulty in monitoring the exact degree of polarization at these energies. We therefore apply the method of flipping the external field.

The spin momentum distribution $J_{\rm mag}(p_z)$ can be analysed by comparison with theoretical distributions obtained from band-structure calculations or by means of atomic electron orbitals. Although the error in using atomic orbitals is important for valence electrons, one may get reasonable agreement with the momentum distribution for core electrons carrying a magnetic moment. Usually, $J_{\rm mag}(p_z)$ is normalized by a known or calculated value for the spin moment. If one aims to determine the absolute value of the spin moment the proportionality factor in the cross section has to be determined. This is performed by a calibration measurement with a known sample under similar experimental conditions, *e.g.* single-crystal Fe gives a strong magnetic signal and has a well determined electron spin moment of $S_{\rm Fe} = 2.07\ \mu_{\rm B}$ (Kubo & Asano, 1990). The spin moment can thus be obtained

$$S = S_{\rm Fe}(mZ^{\rm eff})/(m_{\rm Fe}Z^{\rm eff}_{\rm Fe}) \qquad (2)$$

where $m = (I\uparrow - I\downarrow)/(I\uparrow + I\downarrow)$ is the experimentally determined magnetic effect for the integrated intensities $I\uparrow$ and $I\downarrow$ for both directions of the external field. $Z^{\rm eff}$ is the number of electrons contributing to the Compton profile in the p_z area of interest. In the determination of absolute moments it is important to correct the spectra for additional scattering which reaches the detector. Though intensity from background or multiple scattering does not alter the shape of the difference profile it affects the size of the magnetic effect. To account for multiple scattering a Monte Carlo code adapted to polarized photons by synchrotron radiation (Fajardo *et al.*, 1998) is applied.

3. The experimental set-up

Experiments with photon energies from 80 to 1000 keV have been conducted at the end-station EH *B* of the high-energy beamline ID15 at ESRF and, depending on the photon energy, both avail-

able insertion devices have been used for the experiments described here. The asymmetric wiggler (AMPW) and the superconducting wavelength shifter (SCWS) provide circularly polarized photons above and below the electon orbit plane and using an inclined view to the source these photons can be utilized in magnetic Compton scattering. The spectral flux of highly circular polarized photons (Fig. 1) indicates that the SCWS is the superior device for energies above 150 keV. In the inset of Fig. 1 the vertical fan accepted to obtain $P_c = 0.8$ is indicated. Thick bent-crystal Si monochromators with bending radii ∼60 m are used to assure good energy resolution, high reflectivity and high flux (Suortti *et al.*, 1994). To increase the bandwidth of the incident beam the monochromator can also be used in focusing mode with increased bending (Tschentscher & Suortti, 1998). The photon beam is collimated by slits positioned just before the sample which is mounted in a permanent magnet field. Fig. 2 shows a sketch of the experimental arrangement. Typically, beam sizes of 1 mm horizontal and 2–3 mm vertical are employed. The scattering angle θ is chosen to be very high (150–172°) in order to decrease the resolution component due to geometrical broadening. The large Compton shift of the scattered photon energy leads to a compensation of the incident bandwidth, thereby reducing its contribution to the total resolution. A 13 mm-thick high-purity Ge detector, optimized to achieve a relative resolution of $\sim 4 \times 10^{-3}$ at 122 keV, is used. The efficiency of Ge detectors varies strongly for photon energies above 100 keV and has to be taken into account (Tschentscher & Suortti, 1998). Energy spectra are accumulated with an Ethernet-based multichannel analyser (MCA) and programs to evaluate the magnetic spectra are available.

Depending on effective thicknesses, preferred magnetization directions and available sample dimensions, the experiment can be carried out in transmission or reflection geometry. The sample is placed in the bore of the magnet achieving a field of 0.92 T, which is typically inverted every 30–50 s. The inversion is achieved by a rotation of the whole magnet by means of air pressure. A closed-cycle cryostat adapted to the magnet is available for low-temperature experiments. Depending on the type of study, resolution or higher count rates can be emphasized. In a series of experiments on Fe, the different components contributing to the resolution function have been studied and a program is available to calculate the resolution in order to choose the optimal set-up (McCarthy, Cooper, Honkimäki *et al.*, 1997). Energy resolution and the components due to the bandwidth of the incident photon beam and the geometry can thus be set.

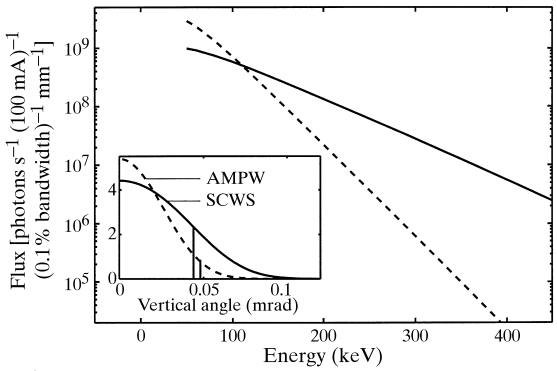

Figure 1
Spectral fluxes of the multipole (broken lines) and superconducting (full lines) insertion devices for circular polarization $P_c = 0.8$. In the inset the vertical flux distribution at $E = 200$ keV is shown and the lines indicate the lower integration limit to achieve $P_c = 0.8$.

4. Experimental results

Experiments have been performed on the transition metals Fe, Ni and Co and on heavy compounds, such as $CeRh_3B_2$ and U compounds. The experiments are described in more detailed publications (see *e.g.* Lawson *et al.*, 1996; Dixon *et al.*, 1998) and we will report only on measurements on Fe and $CeRh_3B_2$ to demonstrate the performance of high-energy magnetic Compton scattering.

4.1. *Fe measurements*

Experiments on Fe have focused on the optimization of the instrument resolution and the ratio of magnetic-to-charge scattering. Measurements at different photon energies varying from 80 to 1000 keV have been used to investigate the cross section for magnetic Compton scattering. The main achievements are a momentum resolution smaller than 0.4 a.u. and an increase in the magnetic effect by a factor of ∼2. The magnetic intensities for photon energies up to 1000 keV have been compared with the Lipps–Tolhoek cross section for a free stationary electron and good agreement was found. The momentum distribution for the Fe 111 direction, measured with a resolution of 0.37 a.u., showed differences in comparison to theoretical calculations, which had not been obtained in earlier experiments with poorer resolution. In Fig. 3 magnetic Compton profiles for the Fe 111 direction at energies from 80 to 720 keV are shown. At lower photon energies the resolution decreases and the magnetic effect becomes less important. At very high photon energies the reduced flux limits the statistical accuracy and the resolution is degraded due to the geometrical resolution component. The best resolution, paired with a high magnetic effect and good statistical accuracy, are found for the energy range 200–250 keV. Results for the resolution function, the cross section and the Fe measurements have been published (McCarthy, Cooper, Lawson *et al.*, 1997; McCarthy, Cooper, Honkimäki *et al.*, 1997).

4.2. *The spin of $CeRh_3B_2$*

$CeRh_3B_2$ is a ternary boride system with an unexpected anomaly for the Curie temperature, whose value of 115 K is much higher than that of other materials of the same class. Experiments with neutrons had estimated the total magnetization of the Ce(4*f*)

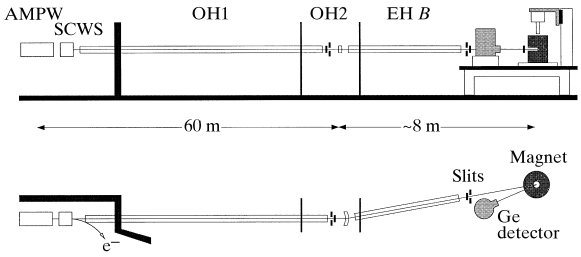

Figure 2
Sketch of the experimental arrangement in a vertical (upper panel) and horizontal cut (lower panel). The beam from the insertion devices (AMPW) is guided in vacuum through the first optics hutch OH1 into OH2, where vertical slits define the degree of circular polarization. In experimental hutch *B* (EH *B*) the monochromated beam strikes the sample which is held in a permanent-magnet field, and scattered photons are detected by a Ge detector in horizontal backscattering geometry.

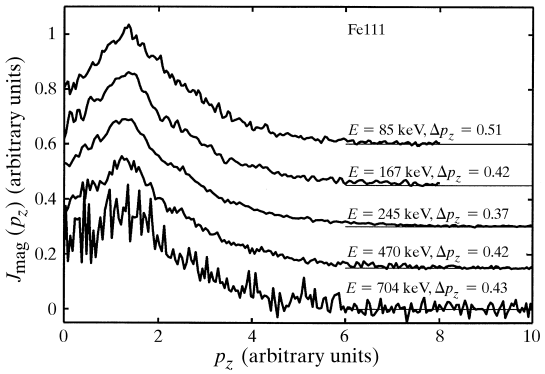

Figure 3
Directional magnetic Compton profiles of Fe for incident energies from 85 to 704 keV. The resolution corresponding to each measurement is indicated. Scattering angles θ, geometrical resolution and incident flux were optimized for each incident energy.

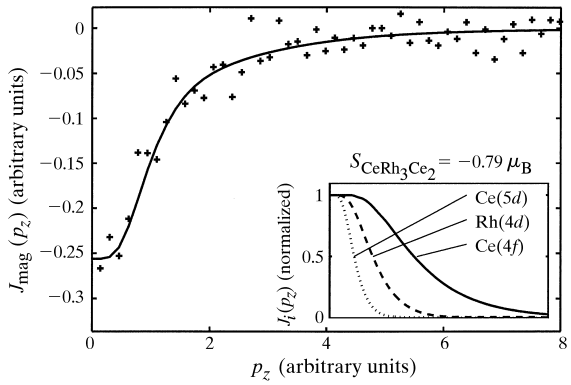

Figure 4
Magnetic Compton profile for $CeRh_3B_2$ in the 100 direction. The sample temperature was 9 K and the total spin magnetic moment is given. The solid line corresponds to a fit of partial momentum distributions obtained from atomic orbitals (Biggs *et al.*, 1975) shown in the insert.

and Ce(5*d*) electrons and had found the magnetization of the Rh(4*d*) state to be negligible (Alonso *et al.*, 1998). Due to the high amount of non-magnetic electrons in this system, the magnetic effect for $CeRh_3B_2$ is ∼25 times smaller than for Fe. The experiment was carried out at $T = 9$ K and it was found that the total spin moment in $CeRh_3B_2$ couples antiferromagnetically with a value of $-0.79\ \mu_B$ (Yaouanc *et al.*, 1998). Fig. 4 shows the fit of atomic orbitals to the magnetic momentum distribution determining the partial moments for Ce(4*f*), Ce(5*d*) and Rh(4*d*). The size and the ferromagnetic coupling of Ce(4*f*) and Ce(5*d*) electrons will have an impact on theoretical models explaining the magnetism in $CeRh_3B_2$.

5. Conclusions

Magnetic Compton scattering at the ESRF is conducted at photon energies much higher than previously available. When energies from 200 to 250 keV are used we achieve a momentum resolution better than 0.4 a.u. and the intensity of the magnetic signal is doubled in comparison to earlier measurements at lower energies. Investigations of the momentum distribution of Fe, Co and Ni have been undertaken and the results have been published. The total spin moment and its partial contributions have been analysed in heavy compounds, where typically very small magnetic effects are seen. To give future access to samples with very small magnetic effects and low internal magnetization it will be necessary to employ a multi-element Ge detector in order to increase the total count rate and a cryomagnet to achieve higher external magnetic fields.

The authors would like to acknowledge very fruitful discussions with M. J. Cooper, University of Warwick, and P. Dalmas de Réotier, A. Yaouanc, CEA, Grenoble. They are indebted to P. Fajardo and M. Sanchez del Rio, ESRF, for provision of the Monte Carlo codes for multiple-scattering and detector efficiency. The rotating permanent magnet was provided by the University of Warwick

References

Alonso, J. A., Boucherle, J. X., Givord, F., Schweizer, J., Gillon, B. & Lejay, P. (1998). *J. Mag. Mag. Mater.* In the press.
Biggs, F., Mendelsohn, L. B. & Mann, J. B. (1975). *Atom. Data Nucl. Data Tab.* **16**, 201–309.
Carra, P., Fabrizio, M., Santoro, G. & Thole, B. T. (1996). *Phys. Rev. B*, **53**, R5994–R5997.
Cooper, M. J., Collins, S. P., Timms, D. N., Brahmia, A., Kane, P. K., Holt, R. S. & Laundy, D. (1988). *Nature (London)*, **333**, 151–153.
Cooper, M. J., Zukowski, E., Collins, S. P., Timms, D. N., Itoh, F. & Sakurai, H. (1992). *J. Phys. Condens. Mater.* **4**, L399-L404.
Dixon, M. A. G., Duffy, J. A., Gardelis, S., McCarthy, J. E., Cooper, M. J., Dugdale, S. B., Jaulborg, T. & Timms, D. N. (1998). *J. Phys. Condens. Matter*, **10**, 2759–2771.
Fajardo, P., Honkimäki, V., Buslaps, Th. & Suortti, P. (1998). *Nucl. Instrum. Methods B*, **134**, 337–345.
Lawson, P. K., Timms, D. N., Dixon, M. A. G., Cooper, M. J., McCarthy, J. E., Hämäläinen, K., Manninen, S. & Tschentscher, Th. (1996). *J. X-ray Sci. Technol.* **6**, 299–307.
Kubo, Y. & Asano, S. (1990). *Phys. Rev. B*, **42**, 4431–4446.
McCarthy, J. E., Cooper, M. J., Honkimäki, V., Tschentscher, Th., Suortti, P., Gardelis, S., Hämäläinen, K., Manninen, S. & Timms, D. N. (1997). *Nucl. Instrum. Methods A*, **401**, 463–475.
McCarthy, J. E., Cooper, M. J., Lawson, P., Timms, D. N., Manninen, S., Hämäläinen, K. & Suortti, P. (1997). *J. Synchrotron Rad.* **4**, 102–109.
McCarthy, J. E., Honkimäki, V., Tschentscher, Th., Shukla, A. & Suortti, P. (1998). In preparation.
Platzman, P. M. & Tzoar, N. (1970). *Phys. Rev. B*, **2**, 3556–3559.
Sakai, N. (1996). *J. Appl. Cryst.* **29**, 81–99.
Sakai, N. & Ôno, K. (1976). *Phys. Rev. Lett.* **37**, 351–353.
Suortti, P., Lienert, U. & Schulze, C. (1994). *Nucl. Instrum. Methods A*, **338**, 27–32.
Suortti, P. & Tschentscher, Th. (1995). *Rev. Sci. Instrum.* **66**, 1798–1801.
Tschentscher, Th. & Suortti, P. (1998). *J. Synchrotron Rad.* **5**, 286–292
Yaouanc, A., de Réotier, P., Sanchez, J.-P., Tschentscher, Th. & Lejay, P. (1998). *Phys. Rev. B*, **57**, R681–R684.